SELECTIVE LASER SINTERING AND POST PROCESSING OF FULLY FERROUS COMPONENTS

Phani Vallabhajosyula and David L. Bourell
Laboratory of Freeform Fabrication
Advanced Manufacturing Center
The University of Texas at Austin
1University Station, MC C2200
Austin, TX 78712-0292
USA

Abstract

Commercially available steel for indirect SLS (LaserForm^{tm} A6 tool steel) is normally post-process infiltrated with a copper-based material. While such parts have high thermal conductivity necessary for short- and medium-run injection molding dies, they are weakened by the second phase with limited high temperature stability. This paper deals with a modification to the commercial process whereby a low-melting-point cast iron is substituted for the copper alloy infiltrant. A predictive model is presented that describes the part equilibrium solid fraction at the infiltration temperature as a function of the green density and infiltration temperature. In an experimental study, green parts were fabricated using LaserForm^{tm} A6 tool steel powder. They were then heated in vacuum to drive off the binder and infiltrated with ASTM A532 white cast iron. During infiltration, an equilibrium state is established between the solid SLS steel part and liquid cast iron associated primarily with carbon diffusion from the cast iron into the tool steel. The equilibrium state is governed by the carbon content of the steel and cast iron, the relative density of the steel part prior to infiltration and the infiltration temperature. In some cases guided by Ashby densification maps, pre-sintering of the tool steel green part was performed to increase the initial relative density of the solid metal.

1. Introduction:

Metal infiltrated metal systems based on selective laser sintering (SLS) have been commercialized for some time [1-5]. High temperature stability of ferrous components demands a stable second phase in the ferrous matrix when compared to the commercial (copper based) infiltrant. Bronze alloy infiltrated SLS green parts [6,7] constitute a relatively weak second phase with limited high-temperature stability. These parts can be used for applications where high thermal conductivity is desired such as short run injection moulds. New infiltrant metals have been considered for which hardness and maximum service temperature are not so severely compromised. In the present work, cast iron is considered as a potential infiltrant for its good fluidity and hardness. Cast iron is also available in a variety of strength grades and microstructures.

This paper deals with the production of fully ferrous components with in-direct selective laser sintering considering cast iron as a potential infiltrant. The methodology involves formation of green part as a result of selective laser sintering of LaserForm^{tm} A6 tool steel powder [8], burnout of the binder and pre-densification of the component followed by infiltration with cast iron. A critical issue is avoiding melting of the tool steel during infiltration. Diffusion of carbon from the cast iron into the tool steel preform results in lowering of the melting point of the tool

steel part significantly. A predictive model is constructed for different infiltration temperatures considering the assumption that it is desirable for the fraction of solid in the final infiltrated part to be equal to or greater than the fraction of solid in the SLS part prior to infiltration. The experimentation and the resulting parts validation for this model are also discussed in detail.

2. Predictive model for infiltration

To ensure the production of a decent infiltrated part, it is critical to set the infiltration temperature such that the solid fraction at equilibrium does not fall too much below the solid fraction of SLS part prior to infiltration. Preferably the equilibrium solid fraction of the final infiltrated part will be greater than the uninfiltrated tool steel part relative density. Hence a predictive model is constructed to determine equilibrium solid fraction at various infiltration temperatures depending on the initial density of the SLS part. The initial density of SLS part prior to infiltration can be varied by sintering the green part at various temperatures.

a) Densification or Ashby plots:

Once the green part is obtained by conventional SLS of the tool steel powder with binder, it is sintered in a vacuum furnace to drive off the binder and create a porous particle network [9]. During the initial stages of sintering coalescence of powder particles occurs by neck formation and growth between the contacting particles. During the intermediate stages particles tend to move closer to one another and the corresponding microstructure is characterized by a tunnel-network of porosity between the particles. Finally the network ceases to exist, giving rise to the formation of isolated spheroidal pores. These pores continue to shrink until the densification is complete. This ensures some hardness to the brown part. The resulting density of the component depends on the initial density, sintering temperature and dwell time at that temperature [10].

Densification of the powder occurs by various mechanisms like plasticity, boundary diffusion, volume diffusion, Nabarro-Herring creep, Coble creep and Power law creep. Ashby, et al. [11, 12] defined densification relations for various mechanisms and created a Temperature Densification Map, a plot of relative density as a function of temperature T. The Ashby plot for densification of LaserForm[tm] A6 Tool steel with initial relative density of 0.48, approximately, is shown in Figure 1. The resulting relative density for the parts sintered at 1100°C for 3hours and 1260°C for 5hrs is marked by points a, b on the plot.
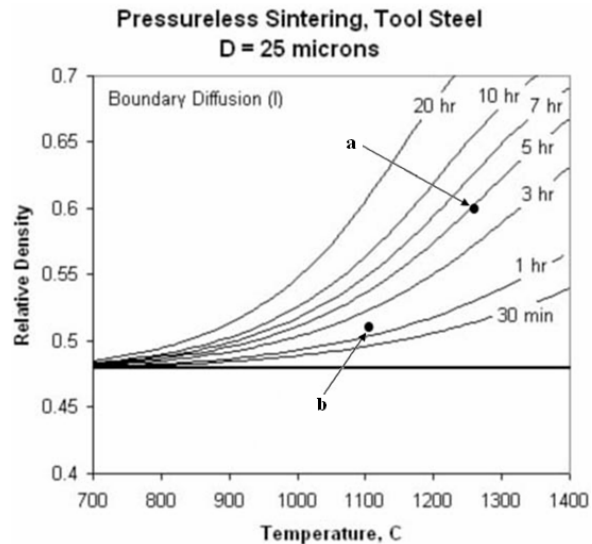

Fig.1. Ashby densification map for tool steel, plotting relative density as a function of temperature and time of sintering. The data points a,b represent increased relative densities of the parts sintered for 3hrs at 1100°C and 5hrs at 1260°C respectively.

b) Equilibrium solid fraction at infiltration temperature:

Infiltration into the brown part should ensure that cast iron melts completely and diffuses into the brown part without disturbing the part geometry. It was hypothesized that the equilibrium state at infiltration temperature is a mixture of solid tool steel and liquid cast iron. A predictive model for infiltration of cast iron into selective laser sintered tool steel is constructed based on the fact that the equilibrium state at the infiltration temperature is governed by i) carbon content of tool steel and cast iron, ii) infiltration temperature, iii) relative density of tool steel SLS part and iv) amount of infiltrant (excess) needed to ensure complete infiltration.

Let C_i and C_m be the carbon composition of cast iron and tool steel respectively. Considering ρ as the density of pure tool steel and cast iron, if Δ is the relative density of the brown tool steel part, the relative density of cast iron to be infiltrated is given by 1-Δ. Let C_e be the equilibrium carbon composition of the resulting part, which may be given by the relation,

$$C_e = [C_m \Delta + C_i (1- \Delta)] = C_i - \Delta (C_i - C_m) \quad \dots (1)$$

As a reference, Figure 2 shows iron-carbon phase diagram with various materials compositions represented [13]. Let C_L and C_S be the carbon compositions of solidus and liquidus lines at equilibrium which in turn depend on infiltration temperature. The equilibrium solid fraction at the infiltration temperature is given by,

Fig. 2. Iron-carbon equilibrium diagram. The definitions for carbon compositions at various points are given in the text.

$$X_e = (C_L - C_e) / (C_L - C_S) = [C_L - C_i + \Delta (C_i - C_m)] / (C_L - C_S) \quad \dots (2)$$

Therefore, the equilibrium solid fraction (X_e) at equilibrium state is a function of relative density of the brown part (Δ) and the infiltration temperature (T_i).

This paper deals with infiltration of SLS tool steel part of carbon composition (C_m) 1.09% (wt) with ASTM A532 Class IA white cast iron of carbon composition (C_i) of 3.56% (wt). Based on Equation (2), a graph predicting the equilibrium solid fraction at various temperatures for different relative densities of the brown part is plotted as shown in Figure 3. The dashed line crossing the curves implies the equilibrium solid fraction is equal to the relative density of the brown part at a given infiltration temperature. A point in Region I i.e., above the dashed line represents a higher value of solid fraction than the value prior to infiltration. The cast iron melts and infiltrates into the solid brown part resulting in a decent fully ferrous component. Any point below the dashed line i.e., in the Region II, represents the equilibrium solid fraction to be actually less than the relative density of the brown part. In this case, melting of the part is observed resulting in the distortion of the part.
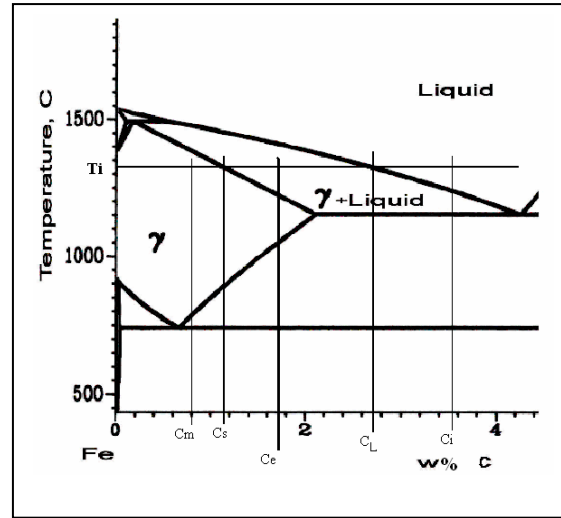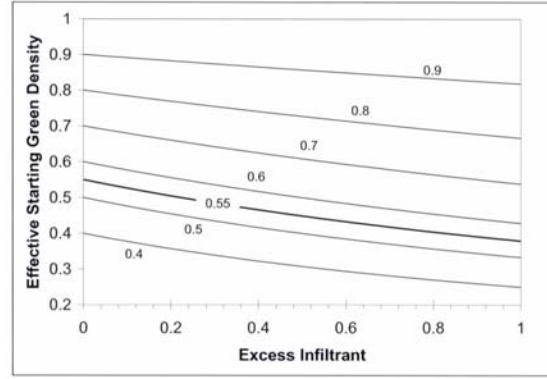
Region I

Region II

Fig.3. Equilibrium solid fraction as a function of infiltration temperature for different densities of brown part. The data points marked on the plot represent figures of various infiltrated parts; the details are discussed in the text.

Fig.4. Effect of excess infiltrant on effective starting density for various densities of tool steel brown part. This also results in a decrease of equilibrium solid fraction at infiltration temperature as the amount of infiltrant increases.

c) Effect of Excess Infiltrant

Excess of infiltrant is needed to ensure complete infiltration of the part. Consider an excess of infiltrant (cast iron) be placed on the tabs of tool steel perform during infiltration. This actually alters the effective solid fraction, decreasing it initially. This in turn decreases the equilibrium solid fraction at infiltration temperature. Let ε be the fraction of excess infiltrant by volume to the actual volume of infiltrant needed i.e., when ε is equal to zero implies the absence of excess infiltrant, and when ε equals to 0.2 implies the volume of infiltrant taken is 20% in excess to the actual volume of infiltrant needed. The effective starting density of green part as a function of excess infiltrant is given by,

$$\Delta_{eff} = \Delta / [\Delta + (1+\varepsilon)(1-\Delta)] = \Delta / [1-\varepsilon(1-\Delta)] \qquad \ldots (4)$$

Figure 4 shows the decrease in the effective starting density as ε increases. The amount of decrease for a reasonable values of $0 < \varepsilon < 0.5$ results in only modest changes to Δ_{eff} of less than 10% approximately.

3. Experimental

Various experiments were carried out to validate the predictive model, in which cubes of dimensions 25mmx25mmx25mm, with a tab for placing the cast iron chunks were built on SLS machine from LaserForm[tm] A6 tool steel. The green density of these SLS parts was obtained from the ratio of weight of the part to its measured volume. Once the green density was known, the part was buried in alumina and put in a furnace to burn out the binder and pre-densify the part. The part was heated at 90°C/hr to a temperature of 750°C to burn out the binder and then at a rate of 100°C/hr to the set temperature, held at that temperature for certain time followed by furnace cooling. The theoretical relative density of the brown part could be predicted from the Ashby plot by knowing the set temperature and the dwell time. This was compared with the actual relative density of the part calculated from its weight and volume.

The pore volume was obtained from the relative density of brown part and the weight of cast iron needed for infiltration was determined. The tab on the brown part was carefully cleaned and cast iron chunks were placed on it for infiltration. The assembly was buried in alumina and placed in furnace. The heating rate was set at 8°C/min up to 650°C and at 100°C/hr up to the

infiltration temperature. The sample was held there for 50 min followed by furnace cooling. Infiltration of the brown parts with different relative densities was carried at different temperatures to validate the above model.

4. Results and Discussion

Various infiltrated parts were obtained from infiltrating brown parts with different initial relative densities at various infiltration temperatures. The geometry of the resulting parts is discussed.

The Green parts from SLS station with a relative density of 0.48 were pre-densified in vacuum at a temperature of 1260°C for 5hours, increasing the relative density to 0.62. Depending on this value of relative density, the weight of cast iron needed for infiltration was calculated. Both the part and the cast iron chunks placed on its tabs were buried in Alumina and set for infiltration at 1190°C. The part shown in Figure 5 is the decent infiltrated part obtained as a result. From the predictive model, it can be seen that at this infiltration temperature, the equilibrium solid fraction of the part is greater than 0.62 which implies no melting of brown part and there by results in an acceptably infiltrated part. The relative density of this part was found to be 0.8. Figure 6 shows another sample, with relative density of brown part being 0.57 and infiltrated at 1230°C. The resulting part with a relative density of 0.64 was sound, thus validating the predictive model.

Fig.5. SLSed A6 tool steel part pre-sintered from a relative density of 0.48 to 0.62 by heating to 1260°C for 5hrs and then infiltrated at 1190°C. The resultant density of infiltrated part was 0.8
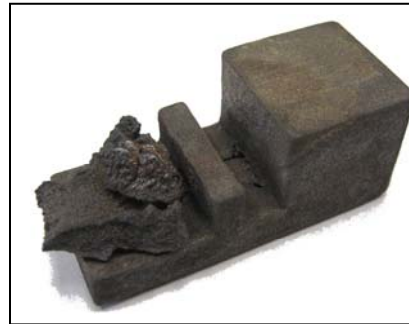
Fig.6. SLSed A6 tool steel part pre-sintered from a relative density of 0.48 to 0.57 by heating to 1260°C for 5hrs and then infiltrated at 1230°C. The resultant density of infiltrated part was 0.64

Fig.7. SLSed A6 tool steel part pre-sintered from a relative density of 0.49 to 0.5 by heating to 1160°C for 3hrs and then infiltrated at 1275°C. Melting of tool stell and hence distortion of the specimen is observed as the infiltration temperature for given brown density lies in Region II

Fig.8. SLSed A6 tool steel part pre-sintered from a relative density of 0.46 to 0.52 by heating to 1100°C for 3hrs and then infiltrated at 1310°C. As the infiltration temperature for given brown density lies in Region II, melting of tool steel along with cast iron is observed, distorting the final part.

183

The part shown in Figure 7 represents a brown part with relative density of 0.5 infiltrated at 1275°C which resulted in melting of tool steel and distorted part geometry. It is evident that selection of infiltration temperature for the given brown part relative density from Region II of the predictive model (Figure 3) resulted in melting of tool steel and distorting the part. The part in Figure 8 also validates the model. Distortion in the final part is observed when a brown part with relative density of 0.52 was infiltrated with cast iron at a temperature of 1310°C. The predictive model also explains the melting of tool steel as the equilibrium solid fraction at this temperature is found to be less than 0.52.

5. Conclusions

A predictive model for infiltration of cast iron into SLS tool steel part was developed and tested for different relative densities of brown parts and at various infiltration temperatures. From the above experiments, it was shown that final parts were consistent with the predictive model, and that fully ferrous components can be obtained by proper selection of infiltration temperature for a given relative density of brown part. The predictive model can be validated further by repeating the experiments at different sintering and infiltration temperatures. Fully dense components might be produced by increasing the number of tabs attached to the part or by adding excess amount of cast iron. The parts obtained should be tested for mechanical properties like hardness, strength and ductility.

REFERENCES

1. J.J. Beaman, J.W. Barlow, D.L. Bourell, R.H. Crawford,H.L. Marcus, K.P. McAlea, "Solid freeform Fabrication: A New Direction In Manufacturing", Kluwer Academic Press, Boston, 1997.

2. R.B. Heady, J.W. Cahn, "An Analysis of the Capillary Forces in Liquid-Phase Sintering Of Spherical Particles", *Met Trans*, 1970, 1#1, 185-189.

3. F.H. Gern, "Interaction Between Capillary Flow and Macroscopic Silicon Concentration in Liquid Siliconized Carbon/Carbon", *Ceramic Trans*, 1995, 58, 149.

4. B. Stevinson, D.L. Bourell, J.J. Beaman, Jr., "Dimensional Stability During Post-processing of Selective Laser Sintered Ceramic Preforms", *Virtual and Rapid Prototyping*, 1#4, 2006, pp. 209-216.

5. B. Stevinson, D.L. Bourell And J.J. Beaman, Jr., "Over-Infiltration Mechanisms in Selective Laser Sintered Si/SiC Preforms", *Rapid Prototyping Journal*, xxx

6. http://www.3dsystems.com/.

7. "Material Guide: Laserform[tm] A6 Steel Materials", 3D Systems, Inc., Rock Hill SC, 2007.

8. Deckard; Carl R. "Method and apparatus for producing parts by selective sintering" United States Patent #4863538, issued September 5, 1989.

9.   David L. Bourell Martin Wohlert and Nicole Harlan, *Deformation, Processing and Properties of Structural Materials,* The Minerals, Metals and Materials Society, 2000.

10. German R.M.(1998) Consolidation Principles and Process Molding in "ASM Handbook Volume 7: Powder Metal Technologies and Applications", ASM International, Materials Park OH USA, 437-452.

11. M.F.Ashby, "A First report on Sintering Maps", Acta Metallurgica, 22(1974) 275-289.

12. F.B.Swinkels and M.F. Ashby, "A Second Report on Sintering Maps", Acta Metallurgica, 29 (1981) 259-281.

13. ASM Handbook, "Volume 3: Alloy Phase Diagrams", 10th ed., ASM International, Materials Park OH, 1992, p. 2.110.